Inelastic neutron scattering study of magnetic excitations in Sr_2RuO_4

M. Braden,[1,2,3,*] Y. Sidis,[2] P. Bourges,[2] P. Pfeuty,[2] J. Kulda,[4] Z. Mao,[5] and Y. Maeno[5,6]
[1]*Forschungszentrum Karlsruhe, IFP, Postfach 3640, D-76021 Karlsruhe, Germany*
[2]*Laboratoire Léon Brillouin, C.E.A./C.N.R.S., F-91191-Gif-sur-Yvette CEDEX, France*
[3]*II. Physikalisches Institut, Universität zu Köln, Zülpicher Straße 77, D-50937 Köln, Germany*
[4]*Institut Laue-Langevin, Boîte Postale 156, 38042 Grenoble Cedex 9, France*
[5]*Department of Physics, Kyoto University, Kyoto 606-8502, Japan*
[6]*International Innovation Center (IIC), Kyoto 606-8501, Japan*
(Received 20 February 2002; published 23 August 2002)

Magnetic excitations in Sr_2RuO_4 have been studied by inelastic neutron scattering. The magnetic fluctuations are dominated by incommensurate peaks related to the Fermi surface nesting of the quasi-one-dimensional d_{xz} and d_{yz} bands. The shape of the incommensurate signal agrees well with random phase approximation calculations. At the incommensurate **Q** positions the energy spectrum considerably softens upon cooling, pointing to a close magnetic instability: Sr_2RuO_4 does not exhibit quantum criticality but is very close to it. ω/T scaling may be fitted to the data for temperatures above 30 K. Below the superconducting transition, the magnetic response at the nesting signal is not found to change in the energy range down to 0.4 meV.

DOI: 10.1103/PhysRevB.66.064522 PACS number(s): 74.70.−b, 78.70.Nx, 75.40.Gb

I. INTRODUCTION

Sr_2RuO_4 is still the only superconducting layered perovskite besides the cuprates;[1] however, in contrast to the cuprate high-temperature superconductors (HTSC's), superconductivity in Sr_2RuO_4 develops in a well-defined Fermi-liquid state.[1,2] Nevertheless, the superconducting state and the pairing mechanism in Sr_2RuO_4 are highly unconventional. The present interest in this compound goes far beyond a simple comparison with the cuprate high-temperature superconductors.

The extreme sensitivity of the superconducting transition temperature on nonmagnetic impurities suggests a nonphonon mechanism.[3] It is further established that superconductivity in Sr_2RuO_4 is made of spin-triplet Cooper pairs and breaks time-reversal symmetry.[2,4] The strongest experimental argument for that can be found in the uniform susceptibility measured either by the NMR Knight shift or polarized neutron experiments[5,6] and in the appearance of spontaneous fields in the superconducting state reported by muon spin resonance (μSR).[7] A spin-triplet *p*-wave order parameter had been proposed before these experiments,[8] in the idea that superconductivity arrises from a dominant interaction with ferromagnetic fluctuations in analogy to superfluid ^{3}He. Rice and Sigrist stressed the comparison with the perovskites $SrRuO_3$ and $CaRuO_3$ which order ferromagnetically or are nearly ferromagnetic, respectively.[9] Evidence for ferromagnetic fluctuations in Sr_2RuO_4 was inferred from NMR experiments: Imai *et al.* found that $1/T_1T$ of the O and Ru NMR exhibit a similar temperature dependence and interpreted that this could be only due to ferromagnetic fluctuations.[10]

The macroscopic susceptibility in Sr_2RuO_4 is enhanced when compared with the band structure calculation but only weakly; in particular, its temperature dependence remains flat.[2,11] There exist also layered ruthenates which are very close to ferromagnetic order at low temperatures: the purest $Sr_3Ru_2O_7$ samples show metamagnetism and samples with somehow less quality even order ferromagnetically.[12] A highly enhanced susceptibility pointing to a ferromagnetic instability is also observed in the phase diagram of $Ca_{2-x}Sr_xRuO_4$,[13,14] but for a rather high Ca concentration, $Ca_{1.5}Sr_{0.5}RuO_4$.[15] In these nearly ordered layered ruthenates, the susceptibility is about two orders of magnitude higher than that in Sr_2RuO_4 and strongly temperature dependent.

Some doubt about the unique role of ferromagnetism in Sr_2RuO_4 arose from the strong-moment antiferromagnetic order observed in the Ca analog,[16] which inspired Mazin and Singh to perform a calculation of the generalized susceptibility based on the electronic band structure.[17] Surprisingly they found that the dominating part is neither ferromagnetic nor antiferromagnetic but incommensurate. The Fermi surface in Sr_2RuO_4 is well studied both by experiment[18] and by theory[19] with satisfactory agreement. Three bands contribute to the Fermi surface which may be roughly attributed to the three t_{2g} levels, the d_{xy}, d_{yz}, and d_{xz} orbitals, occupied by the four $4d$ electrons of Ru^{4+}. The d_{xy} orbitals hybridize in the xy plane and, therefore, form a band with two-dimensional character, the γ-band. In contrast, the d_{xz} and d_{yz} orbitals may hybridize only along the x and y directions, respectively, and form quasi-one-dimensional bands, the α and β bands, with flat sheets in the Fermi surface, the α and β sheets. The latter give rise to strong nesting and enhanced susceptibility for $\mathbf{q}=(0.33,q_y,0)$ or $\mathbf{q}=(q_x,0.33,0)$.[17] Along the diagonal both effects strengthen each other, yielding a pronounced peak in the susceptibility at $\mathbf{q}_{i-\mathrm{cal}}=(0.33,0.33,0)$. Using inelastic neutron scattering (INS) we have perfectly confirmed this nesting scenario.[20] The dynamic susceptibility at moderate energies is indeed dominated by the incommensurate fluctuations occurring very close to the calculated position at $\mathbf{q}_i=(0.30,0.30,0)$. Furthermore, we found a pronounced temperature dependence which can explain the temperature dependence of both Ru and O $1/T_1T$ NMR.[10]

In the meanwhile, several groups have worked on theories where superconductivity is related to the incommensurate fluctuations.[21–23] These theories, however, do not yet give an explanation for the fine structure of the order parameter. Specific heat data on the highest-quality samples clearly indicate the presence of line nodes in the superconducting state.[24] Ultrasonic[25] and thermal conductivity[26] results would disagree with vertical line nodes, which leaves horizontal line nodes as the only possible ones. Zhitomirsky and Rice[27] assume that superconductivity is transferred from the γ band to the α and β bands by a proximity effect and get a conclusive explanation for the horizontal line nodes. In this model superconductivity should be mainly related to excitations associated with the active γ band, which so far have not been characterized. Therefore, it appears still interesting to further deepen the study of the magnetic fluctuations in Sr_2RuO_4.

In this paper we report on additional INS studies in Sr_2RuO_4 in the normal as well as in the superconducting phase. We present a more quantitative analysis of the incommensurate fluctuations related to the α and β sheets and discuss the possible contributions due to the two-dimensional γ band.

II. EXPERIMENT

A. Experimental setup

Single crystals of Sr_2RuO_4 were grown by a floating zone method in an image furnace; they exhibit the superconducting transition at $T_c=0.7$, 1.35, and 1.43 K and have volumes of about 450 mm^3 each. Since most of the measurements were performed in the normal phase, where the differences in T_c should not affect the magnetic excitation spectrum, we aligned the three crystals together in order to gain counting statistics in the INS experiments. Count rates in the ruthenates experiments are relatively small already due to the steeper decrease of the Ru magnetic form factor with increasing scattering vector. For the measurements below and across the superconducting transition we mounted only the two crystals with relatively high T_c together. The mounting of the two or three crystals was achieved with individual goniometers, yielding a total mosaic spread below 0.5°.

We used the thermal triple-axis spectrometer 1T installed at the Orphée reactor (Saclay, France) in order to further characterize the scattering in the normal state. The instrument was operated with a double-focusing pyrolithic graphite (PG) monochromator and analyzer; in addition, PG filters in front of the analyzer were used to suppress higher-order contamination, the final neutron energy being fixed at 14.7 meV. All diaphragms determining the beam paths were opened more widely than usual in order to relax the **Q** resolution, since the magnetic signals are not sharp in **Q** space. In most experiments, the scattering plane was defined by (1,0,0) and (0,1,0) directions in order to span any directions within the (ab) plane. An additional experiment has been made with the (1,1,0) and (0,0,1) directions oriented in the plane to follow the spin fluctuations along the c^* axis.

Studies aiming at a response in the magnetic excitation spectrum on the opening of the superconducting gap require an energy resolution better than the expected value for twice the superconducting gap. Therefore, such an experiment is better placed on a cold triple-axis spectrometer even though this implies a sensitive reduction in the flux. We have made preliminary studies using the cold spectrometers 4F at the Orphée reactor and a more extensive investigation on the spectrometer IN14 at the ILL. These instruments possess PG monochromators (double at 4F and focusing at IN14) and focusing analyzers. The final neutron energy was fixed at $E_f=5$ meV on both cold source spectrometers where a Be filter has been employed to cut down higher-order wavelength neutrons. Cooling was achieved by use of a dilution and a He^3 insert at 4F and IN14, respectively.

B. Theoretical background for magnetic neutron scattering

The magnetic neutron cross section per formula unit is written in terms of the Fourier transform of the spin correlation function $S_{\alpha\beta}(\mathbf{Q},\omega)$ (labels α,β correspond to x,y,z) as[28]

$$\frac{d^2\sigma}{d\Omega d\omega}=\frac{k_f}{k_i}r_0^2F^2(\mathbf{Q})\sum_{\alpha,\beta}\left(\delta_{\alpha,\beta}-\frac{Q_\alpha Q_\beta}{|\mathbf{Q}|^2}\right)S_{\alpha\beta}(\mathbf{Q},\omega), \tag{1}$$

where k_i and k_f are the incident and final neutron wave vectors, $r_0^2=0.292$ b, and $F(\mathbf{Q})$ is the magnetic form factor. The scattering vector **Q** can be split into $\mathbf{Q}=\mathbf{q}+\mathbf{G}$, where **q** lies in the first Brillouin zone and **G** is a zone center. All reciprocal space coordinates (Q_x,Q_y,Q_z) are given in reduced lattice units of $2\pi/a$ or $2\pi/c$.

According to the fluctuation-dissipation theorem, the spin correlation function is related to the imaginary part of the dynamical magnetic susceptibility times the by one enhanced Bose factor:

$$S_{\alpha\beta}(\mathbf{Q},\omega)=\frac{1}{\pi(g\mu_B)^2}\frac{\chi''_{\alpha\beta}(\mathbf{Q},\omega)}{1-\exp(-\hbar\omega/k_BT)}. \tag{2}$$

In case of weak anisotropy, which is usually observed in a paramagnetic state, $\chi''_{\alpha\beta}(\mathbf{Q},\omega)$ reduces to $\chi''(\mathbf{Q},\omega)\delta_{\alpha,\beta}$. Note that for itinerant magnets, anisotropy of the susceptibility can occur due to spin-orbit coupling. $F(\mathbf{Q})$ can be described by the Ru^+ magnetic form factor in a first approximation. Once determined, the magnetic response is converted to the dynamical susceptibility and calibrated in absolute units by comparison with acoustic phonons, using a standard procedure depicted in Ref. 20.

III. RESULTS AND DISCUSSION

A. RPA analysis of the magnetic excitations

At low temperature Sr_2RuO_4 exhibits well-defined Fermi-liquid properties; therefore, it seems appropriate to assess its magnetic excitations within a random phase approximation (RPA) approach based on the band structure. Density functional calculations in local density approximation (LDA) were performed by several groups and yield good agreement with the Fermi surface determined in de Haas–van Alphen

experiments. The bare noninteracting susceptibility $\chi^0(\mathbf{q})$ can be obtained by summing the matrix elements for an electron hole excitation:[28]

$$\chi^0(\mathbf{q},\omega) = -\sum_{\mathbf{k},i,j} M_{\mathbf{k}i,\mathbf{k}+\mathbf{q}j} \frac{f(\varepsilon_{\mathbf{k}+\mathbf{q},j}) - f(\varepsilon_{\mathbf{k},i})}{\varepsilon_{\mathbf{k}+\mathbf{q},j} - \varepsilon_{\mathbf{k},i} - \hbar\omega + i\epsilon}, \quad (3)$$

where $\epsilon \to 0$, f is the Fermi distribution function, and ε_k is the quasiparticle dispersion relation. This was first calculated by Mazin and Singh[17] under the assumption that only excitations within the same orbital character are relevant (the matrix elements $M_{\mathbf{k}i,\mathbf{k}+\mathbf{q}j}$ are equal to 1 or 0). Mazin and Singh predicted the existence of peaks in the real part of the bare susceptibility at $\omega=0$ due to the pronounced nesting of the α and β bands. These peaks were calculated at (0.33,0.33,0) and experimentally confirmed very close to this position at $\mathbf{q}_i=(0.3,0.3,0)$; see Fig. 1. In addition to the peaks at $\mathbf{q}_i$, this study finds ridges of high susceptibility at (0.3, q_y,0) for $0.3<q_y<0.5$ and some shoulder for $0<q_y<0.3$.

The susceptibility gets enhanced through the Stoner-like interaction which is treated in the RPA by

$$\chi(\mathbf{q}) = \frac{\chi^0(\mathbf{q})}{1 - I(\mathbf{q})\chi^0(\mathbf{q})}, \quad (4)$$

with the **q**-dependent interaction $I(\mathbf{q})$. For the nesting positions Mazin and Singh get $I(\mathbf{q})\chi^0(\mathbf{q})=1.02$, which already implies a diverging susceptibility and a magnetic instability.

In Fig. 1 we show a scheme of the $(hk0)$ plane in reciprocal space. Due to the body centering in space group $I4/mmm$ any (hkl) Bragg points have to fulfill the condition $(h+k+l)$ even; (100), for instance, is not a zone center but a Z point. The boundaries of the Brillouin zones are included in the figure. Large solid circles indicate the position of the incommensurate peaks as predicted by the band structure and as observed in our previous work. The thick lines connecting four of them correspond to the ridges of enhanced susceptibility also suggested in Ref. 17.

In the meanwhile several groups have performed similar calculations which all agree on the dominant incommensurate fluctuations.[23,29–32] However, there are serious discrepancies concerning the detailed structure of the spin susceptibility away from $\mathbf{q}_i$. These discrepancies mainly rely on the parameters used to describe the electronic band structure, on the choice of $I(\mathbf{q})$, and on the inclusion of more subtle effects such as spin-orbit or Hund couplings.

In order to compare directly to the INS experiments [see Eqs. (1) and (2)], it is necessary to perform the RPA analysis by taking into account both real and imaginary parts of the susceptibility. Morr *et al.*[32] report such calculations obtained by fitting the band structure to the angle-resolved photoemission spectroscopy (ARPES) results.[33] They find in addition to the peak at $\mathbf{q}_i$ a quite strong intensity near $\mathbf{P}_i=(0.3,0.5,0)$ (the middle of the walls; see Fig. 1), which is even comparable to that at $\mathbf{q}_i$ in the bare susceptibility. Similar results were obtained in Refs. 23 and 29. Ng and Sigrist[30] find much less spectral weight in the ridges at (0.3, q_y) for $0.3<q_y<0.5$ but stronger shoulders $0<q_y<0.3$. In addition,

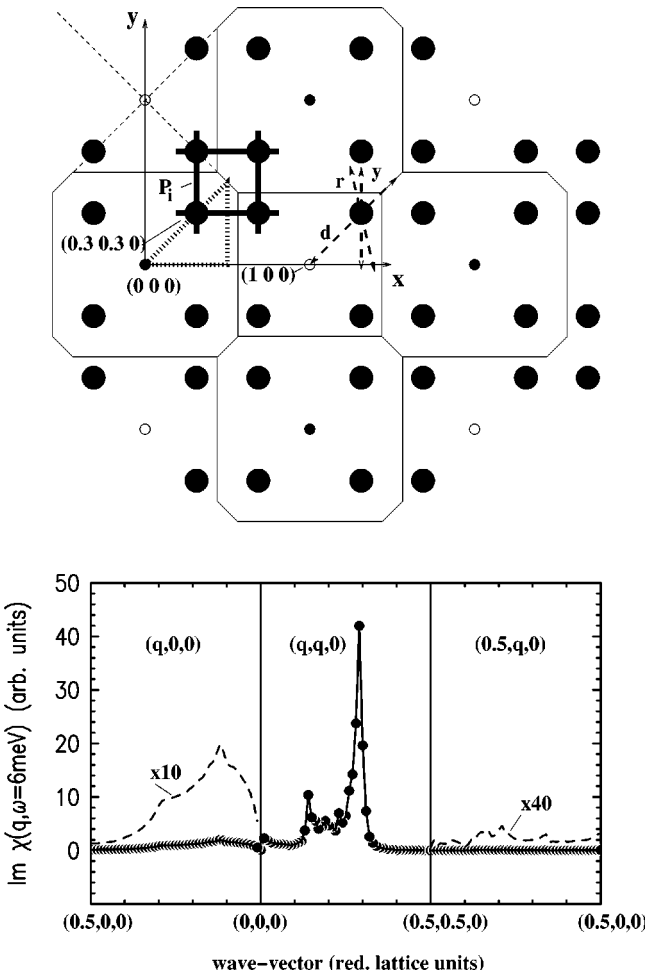

FIG. 1. Upper part: scheme of the $(hk0)$ plane in reciprocal space. Thin lines show the boundaries of the Brillouin zones and small solid and open circles the zone centers and Z points of the body-centered lattice. Large solid circles indicate the position of the incommensurate peaks, and the thick lines connecting four of them correspond to the walls of enhanced susceptibility also suggested in Ref. 17. The dashed double arrows show the paths of the constant energy scans frequently used in this work: along the [010] direction, **y** scan; transverse to the **Q** vector, **r** scan; and along the diagonals in the [110] direction, **d** scans. Lower part: imaginary part of the generalized susceptibility calculated by the RPA along the three paths indicated in the upper part as dotted lines.

they calculate the separate contribution of the γ band which does not show a particular enhancement in the ferromagnetic **q** range but is little structured. Eremin *et al.*[31] calculated the susceptibility, taking into account strong hybridization, and obtained results somehow different from the other groups. They find a strong signal at $\mathbf{P}_i$; in addition, there is some enhancement of the susceptibility related to the van Hove singularity of the γ band. This contribution occurs quite close to the zone center at $\mathbf{q}_{\mathrm{vH}}=(0.15,0,0)$.

We have performed the full RPA analysis basing on the LDA band structure reported in Refs. 17 and 19 in order to accompany our experimental investigations. We first calculate the bare electron hole susceptibility χ^0 from the usual expression, Eq. (3). For the band energies $\epsilon(k_x,k_y,k_z)$ we

use the expressions of Mazin and Singh[19] for the three mutually nonhybridizing tight-binding bands in the vicinity of the Fermi level:

$$\epsilon_{xy}(k_x,k_y,k_z)=400\ \text{meV}\{-1-2[\cos(k_x)+\cos(k_y)] - 1.2\cos(k_x)\cos(k_y)\}, \quad (5)$$

$$\epsilon_{xz}(k_x,k_y,k_z)=400\ \text{meV}[-0.75+1.25\cos(k_x) - 0.5\cos(k_x/2)\cos(k_y/2)\cos(k_z/2)], \quad (6)$$

$$\epsilon_{yz}(k_x,k_y,k_z)=400\ \text{meV}[-0.75+1.25\cos(k_y) - 0.5\cos(k_x/2)\cos(k_y/2)\cos(k_z/2)]. \quad (7)$$

We also used the crude approximation that matrix elements for transitions between bands of the same character are equal to 1 and others 0. The **q**-dependent ''ferromagnetic'' interaction (Stoner factor) $I(\mathbf{q})$ is taken to be equal to (following Ref. 17) $I(\mathbf{q})=(320\ \text{meV})/(1+0.08\mathbf{q}^2)$. With this choice of $I(\mathbf{q})$ the calculated static susceptibility $\chi(\mathbf{q}=0,\omega=0)$ is slightly lower than the measured one. If $I(\mathbf{q})$ is chosen larger, an instability appears at the incommensurate wave vector.

Our results for the imaginary part of the generalized susceptibility at an energy transfer of 6 meV are given in the lower part of Fig. 1. Besides the dominating nesting peak near $\mathbf{q}_i$ there is a further contribution near (0.15,0.15,0) which is related to the γ sheet. In contrast we find a small susceptibility near $\mathbf{P}_i$ and for $(q_x,0,0)$ with small values of q_x.

Since the **q** position of the magnetic excitations was found not to depend on energy, it is easiest to observe the signal in INS by scanning at constant energy. The scan paths are included in Fig. 1; they are purely transverse or rocking like, **r** scan; along a [100] direction, **x** scans; and in a diagonal direction, **d** scans.

The observed signal is rather broad and, therefore, the scans performed are extremely wide, covering complete cuts through the Brillouin zone. This further implies that the background (BG) may be nonconstant, at least sloping. Also, the signals are relatively weak compared to typical triple-axis spectrometry problems; this implies that sample-independent BG contributions which usually are negligible play a role. Figure 2 presents the results of **d** scans at different temperatures, clearly demonstrating the gain in statistics compared to the previous work.[20] The magnetic intensity shown in Fig. 2 disappears upon heating but this effect gets partially compensated for by the gain through the Bose factor.

B. Shape of the incommensurate signal

The fact that the incommensurate signal around a zone center and around a *Z* point, (001), are equivalent already indicates that the coupling between RuO_2 planes is negligible, i.e., that in-phase and out-of-phase couplings are indistinguishable. The two-dimensional (2D) character has been directly documented by Servant *et al.*[34] who found no q_l dependence at $(0.3,0.3,q_l)$ for q_l between -0.5 and 0.5. We find the same result by varying Q_l in a broader range between 2 and 5 in $(0.3,0.3,Q_l)$; see Fig. 3. This 2D character is actually surprising since the dispersion relation of the quasiparticles involved in the computation of $\chi''(\mathbf{q},\omega)$ is not purely 2D.[17] One may therefore expect weak spin correlation along the c^* direction.

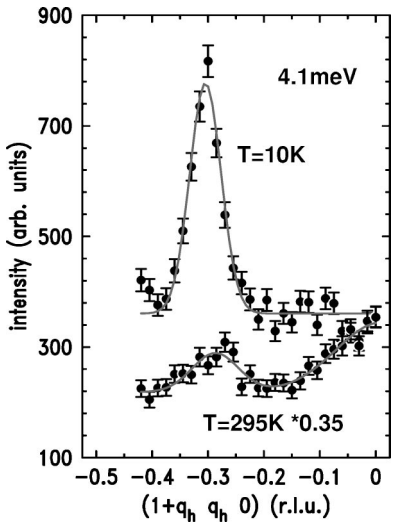

FIG. 2. **d** scans across the incommensurate peak $Q=(0.7,-0.3,0)$ at low and high temperatures; the data at 295 K were scaled by 0.35. The disappearance of the signal upon heating gets partially compensated by the gain through the Bose factor.

Recently, it has been shown that these fluctuations freeze out into a spin-density-wave (SDW) ordering by a minor replacement of Ru by Ti.[35] In this ordering a very short correlation length along the *c* direction nicely reflects the 2D character of the incommensurate inelastic signal. The SDW propagation vector finally favored in the static ordering corresponds to the out-of-phase coupling between neighboring layers. This static interlayer coupling might be even due to the CDW always coupled to a SDW, which, however, has not yet been discovered so far. One may add that the stripe ordering in $La_{1.67}Sr_{0.33}NiO_4$, which differs from the

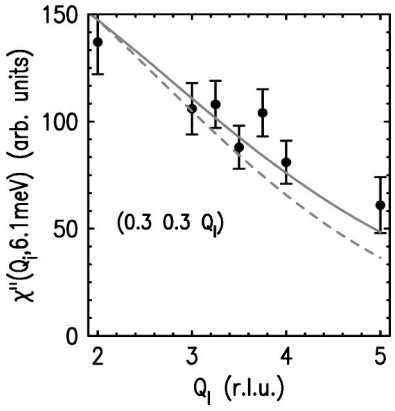

FIG. 3. Height of the magnetic signal at the incommensurate position as function of Q_l; the dashed line shows the dependence expected from the Ru^+ form factor and the solid line that assuming the spin-density distribution observed recently in $Ca_{1.5}Sr_{0.5}RuO_4$(Ref. 39); see text.

$Sr_2Ru_{1-x}Ti_xO_4$ case in many aspects, but nevertheless may be considered as a mixed SDW-CDW ordering, occurs at the same propagation vector.[36]

The wider Q_l dependence of the incommensurate signal shown in Fig. 3 can give information about the anisotropy of the excitation, since INS measures only the spin component perpendicular to Q. We consider the diagonal susceptibility $\chi''_{\alpha\beta}$ with tetragonal symmetry $\chi_\pm := \chi''_{xx} = \chi''_{yy} \neq \chi''_{zz}$. The measured intensity is then given by

$$\frac{d^2\sigma}{d\Omega d\omega} \propto F^2(\mathbf{Q}) \left[\left(1 - \frac{Q_l^2}{|\mathbf{Q}|^2} \right) \chi''_{zz} + \left(1 + \frac{Q_l^2}{|\mathbf{Q}|^2} \right) \chi''_{\pm} \right], \quad (8)$$

which implies that the observations at high Q_l favor the in-plane component of the susceptibility. For a detailed analysis, one has to compare with the form factor. In the figure we show the Q_l dependence assuming that the spin density is localized at the Ru site and may be modeled by the form factor of Ru^+.[37] The Ru form factor dependence underestimates the signal at higher Q_l values; however, the Ru^+ form factor is certainly a too crude approximation. Measurements of the spin-density distribution induced by an external field have not been very precise due to the small magnetic susceptibility and the resulting small moment in Sr_2RuO_4.[38] However, in $Ca_{1.5}Sr_{0.5}RuO_4$ which exhibits ferromagnetic ordering below 1 K and whose low-temperature susceptibility is about two orders of magnitude higher than that in Sr_2RuO_4,[13–15] it has been possible to study the field-induced spin-density distribution. These experiments revealed an extremely high amount of spin density at the oxygen position, about one-third of the total moment,[39] and an orbital contribution at the Ru site. By use of the $Ca_{1.5}Sr_{0.5}RuO_4$ spin-density distribution one obtains a good description of the Q_l dependence given in Fig. 3. However, the form factor in Sr_2RuO_4 should be even more complex. Since the main contribution originates from the flat d_{xy} orbitals,[31] there must be an anisotropy in the effective form factor which indeed was observed in $Ca_{1.5}Sr_{0.5}RuO_4$.[39] Qualitatively, the anisotropy in the form factor has to be compensated for by some weak anisotropy in the spin susceptibility, i.e., by an enhanced out-of-plane component. Such a susceptibility anisotropy corresponds to the orientation of the spins in the SDW ordering phase in $Sr_2Ru_{1-x}Ti_xO_4$,[35] where the spins are aligned parallel to the c direction, and also to the conclusion deduced by Ng and Sigrist from the influence of spin-orbit coupling in Sr_2RuO_4.[30]

Shoulder of the incommensurate peak. In order to examine the shape of the incommensurate peak and to verify the existence of the ridges of additional nesting intensity or the additional peak $\mathbf{P}_i$, reported in different band structure analyzes,[17,29–32] we have scanned across $\mathbf{q}_i$ along the [100] or [010] directions, **y** scans; see Fig. 1. The results are shown in Fig. 4. One can recognize that the incommensurate peak is not symmetric but exhibits always a shoulder to the lower q_x side in absolute units. The shoulder is seen in many scans in reversed focusing conditions of the spectrometer configuration excluding an experimental artifact. Our full RPA calculation nicely agrees with such shoulder; the thin line in Fig. 4 shows the calculated imaginary part of the susceptibility at the energy transfer of the scan and describes the observed signal perfectly besides a minor offset in the position of the incommensurate signal. In contrast, neither the experiment nor our full RPA analysis yields significant intensity in the ridges, i.e., the range $(q_x,0.3,0)$ with $0.3<q_x<0.5$; see Figs. 1 and 4. In particular an intensity at P_i only 3 times weaker than that at $\mathbf{q}_i$ would have been easily detected experimentally. The nesting peak appears to be isolated with two shoulders along [100] and [010] to the lower absolute $q_{x,y}$ sides. These shoulders are connected to the γ sheet.

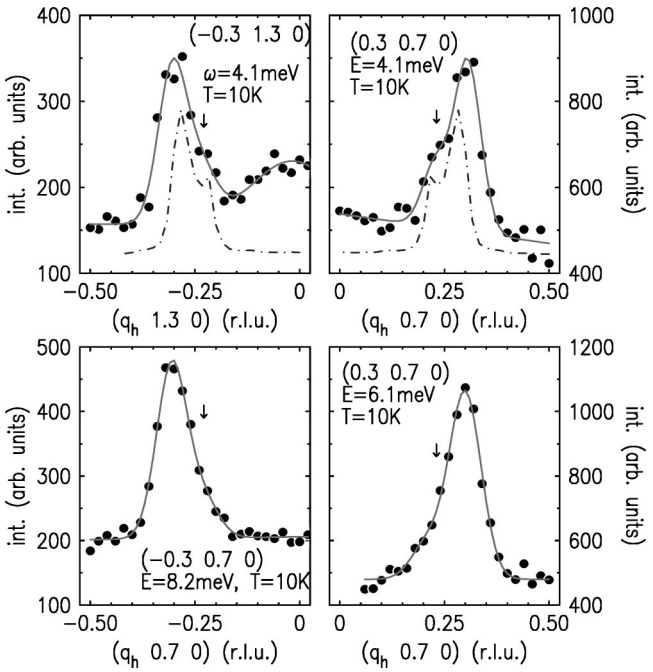

FIG. 4. Results from constant energy scans across the incommensurate position along the [100] direction. Solid lines denote fits with Gaussians and dashed lines the calculated imaginary part of the generalized susceptibility at the energy of 4.1 meV (shifted in the y axis). Arrows indicate the position of the shoulder seen in the RPA calculations.

C. Possible additional magnetic excitations

In none of the band structure calculations one finds evidence for a strong and sharp enhancement of any susceptibility exactly at the zone center pointing to a ferromagnetic instability.[17,29–32] However, several of these calculations find some large susceptibility near the zone center which can be associated with the van Hove singularity of the γ band closely above the Fermi level. Eremin *et al.*[31] report this signal at $\mathbf{q}=(0.1–0.2,0,0)$; other groups find a small peak along the diagonal $(q,q,0)$.[23,29,30] Our own analysis also yields such a signal which is found to be strongest at (0.15,0.15,0) and which levels out along the [100] and [010] directions; see Fig. 1.

In order to address this problem we have mapped out the intensity for $(Q_x,Q_y,0)$ with $-0.5<Q_x<-0.0$ and $0.6<Q_y<1.5$; these scans are shown in Fig. 5 after subtraction of the scattering-angle-dependent background. It is obvious that the incommensurate peak is by far the strongest signal.

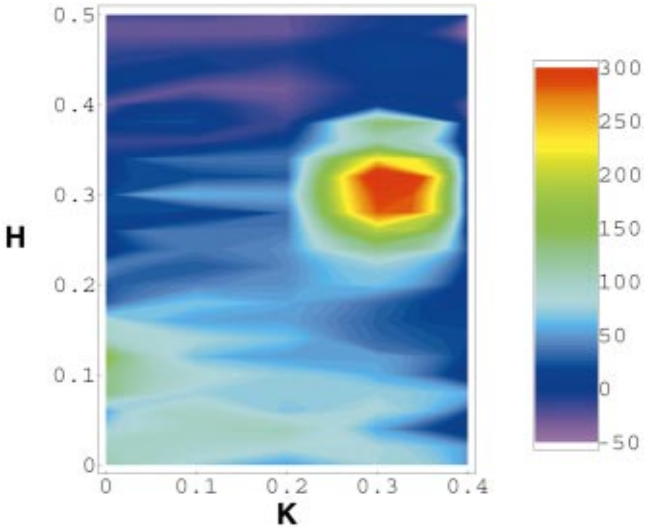

FIG. 5. (Color) Mapping of the INS intensity by constant energy scans with fixed Q_y at 4.1 meV energy transfer. The color plot was obtained by adding symmetrical data after subtraction of the scattering-angle-dependent background.

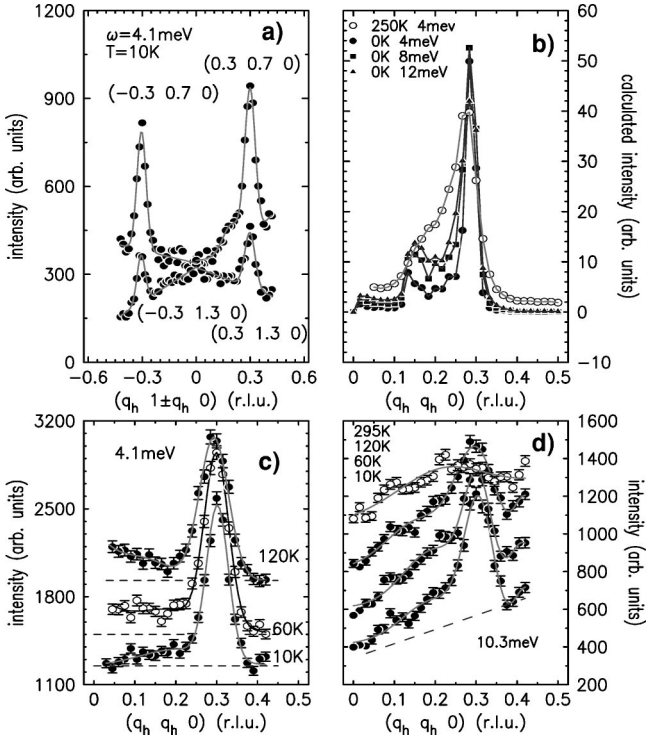

FIG. 6. (a) Scans across the four incommensurate spots surrounding $\mathbf{Q}=(0,1,0)$ in the diagonal direction. (b) Calculated intensity (corresponding to the imaginary part of the susceptibility multiplied by the thermal factor) at different temperatures and energies. (c) Sum of the four scans shown in part (a) for different temperatures at $\omega=4.1$ meV. (d) Sum of the four scans shown in part (a) at $\omega=10.3$ meV (at 295 K not all four scans have been performed).

At low temperature one may roughly estimate any additional signal to be at least a factor of 6 smaller than the nesting peak. The analysis of such weak contributions is quite delicate and demands a reliable subtraction of the background. Nevertheless, the scans in Fig. 5 indicate some scattering closer to the zone center. However, this contribution is not sharply peaked at the Γ point but forms a broad square or a circle. The signal roughly agrees with the prediction that the γ band yields magnetic excitations near the zone center.

Since the sloping background is a major obstacle to analyze the additional contributions, we tried to compensate for these effects by scanning from $\mathbf{Q}=(010)$ along the four diagonals, which are illustrated in Fig. 1, and by summing the four scans. The results are given in Fig. 6. In the four single scans [Fig. 6(a)], one recognizes the nesting signal with its intensity being determined by the form factor and the sloping background. The summed scans [see Fig. 6(c)] should have constant background and the low-temperature summed scan once more documents that the nesting signal is by far the strongest one. However, upon heating additional scattering contributions seem to become enhanced in intensity in particular compared to the nesting signal which decreases; note that the Bose factor will already strengthen any signal by a factor of 3 in the data in Fig. 6(c). Also, at higher energy the additional scattering seems to be stronger as seen in Fig. 6(d) (the background is strongly sloping even in the sum due to a smaller scattering angle). The energy and temperature dependence of the additional contribution corresponds to that predicted by the full RPA analysis for the γ-band magnetic contribution shown in Fig. 6(b). The spectral weight at $\mathbf{Q}=(0.15,0.15,0)$ relative to that of the nesting feature increases upon increasing temperature or energy as is expected for a signal directly related to the van Hove singularity. Due to the agreement between the INS results and the RPA calculations, we suggest to interpret the additional broad scattering as being magnetic in origin; however, a polarized neutron study would be highly desirable. This scattering further might be relevant for a quantitative explanation of the NMR data,[10,20] in particular its temperature-independent part.

Sr_2RuO_4 is not close to ferromagnetic order but substitution of Sr through Ca yields such order for the concentration $Ca_{1.5}Sr_{0.5}RuO_4$.[15] This doping effect was explained in a band structure calculation[40] as arising from a downshift in energy of the γ band pushing the van Hove singularity closer to the Fermi level. In such samples the γ-band magnetic scattering should therefore become strongly enhanced. Indeed first INS studies on these compounds reveal broad signals similar to the additional scattering described above, but much stronger.[41] This strongly supports a magnetic interpretation of the scattering in Figs. 5 and 6.

D. Combined temperature and energy dependence of the incommensurate signal

The energy and temperature dependence has been studied in more detail by performing **r** scans across the incommensurate position, since in this mode the background is almost flat. However, due to phonon contributions, we could not extend the measurements to energies higher than 12 meV, which is slightly below the lowest phonon frequency observed at $\mathbf{q}_i$.[42] In particular the large scans required to cover

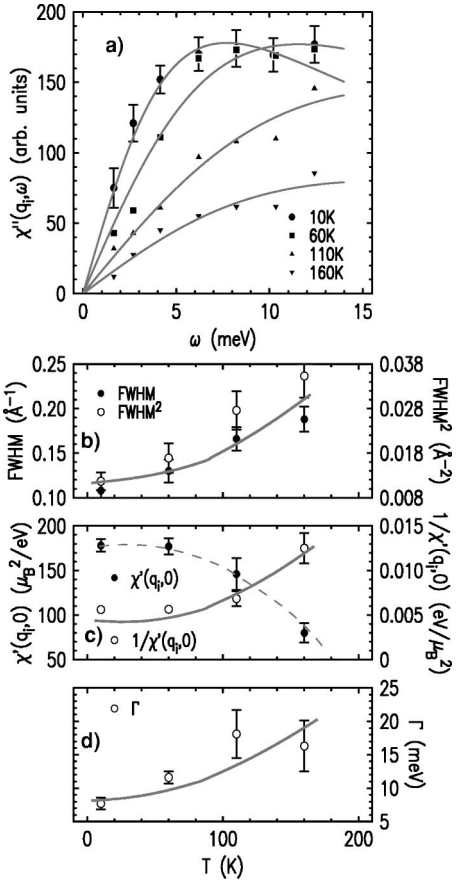

FIG. 7. Observed imaginary part of the generalized susceptibility as function of energy and temperature; lines are fits with a single relaxor (a). Temperature dependence of the averaged full width at half maximum (FWHM) corrected for the experimental resolution and temperature dependence of the square of the FWHM (b). Temperature dependence of the amplitude and its inverse (c) and of the characteristic energy (d) in the relaxor behavior fitted to part (a). Lines in (b)–(d) are guides to the eye.

the broad magnetic signal prevent any analysis within the phonon band frequency range on a nonpolarized thermal triple-axis spectrometer.

The results of the scans are given in Fig. 7. At low temperature we find an energy spectrum in good agreement to that published earlier.[20] In the range up to 12 meV we observe at all temperatures an energy-independent peak width, which, however, increases upon increase of temperature. For temperatures much higher than 160 K the background considerably increases (see Fig. 2) and prevents a detailed analysis within reasonable beam time. In Fig. 7(b) we show the temperature dependence of the peak width averaged over the different energies which agrees well with the results obtained from the single scans with less statistics reported in Ref. 20. Even at the lowest temperature the width of the signal remains finite.

The spectral functions have been fitted by a single-relaxor behavior:[43]

$$\chi''(\mathbf{q}_i,\omega)=\chi'(\mathbf{q}_i,0)\frac{\Gamma\omega}{\omega^2+\Gamma^2}, \tag{9}$$

where Γ is the characteristic energy and $\chi'(\mathbf{q}_i,0)$ the amplitude which corresponds to the real part of the generalized susceptibility at $\omega=0$ according to the Kramers-Kronig relation. The **Q** dependence of the signal may be described by a Lorentzian distribution with half width at half maximum κ, but due to experimental broadening the constant energy scans are equally well described by Gaussians. At low temperature the spectrum clearly exhibits a characteristic energy as seen in the maximum of the energy dependence, but this maximum is shifted to higher values upon heating. Figures 7(c) and 7(d) report the results of the least-squares fits with the single relaxor. Although the statistics is still limited, the tendencies can be obtained unambiguously. The height of the spectral functions $\chi'(\mathbf{q}_i,0)$ rapidly decreases upon heating, which overcompensates the broadening of the signal in **Q** space.

Our finding that the characteristic energy in the range 6–9 meV is well defined only at low temperatures can be related with the far-infrared *c*-axis reflectance study by Hildebrand *et al.*,[44] since the optical spectrum shows a feature in this energy range at low temperatures. In Ref. 20 we have compared the temperature dependence of the incommensurate signal with that of the spin-lattice relaxation rate T_1 measured by both ^{17}O and ^{101}Ru NMR experiments.[10] These NMR techniques probe the low-energy spin fluctuations ($\omega\rightarrow 0$ with respect to INS measurements); furthermore, they integrate the fluctuations in **q** space. $(1/T_1T)$ is related to the generalized susceptibility and the INS results by[45]

$$(1/T_1T)\simeq\frac{k_B\gamma_n^2}{(g\mu_B)^2}\sum_q\left|A(\mathbf{q})\right|^2\frac{\chi''(\mathbf{q},\omega)}{\omega}\Bigg|_{\omega\rightarrow 0}, \tag{10}$$

with $|A(\mathbf{q})|$ the hyperfine fields. $(1/T_1T)$ corresponds hence to the slope of the spectral function in Fig. 7(a) times the extension of the signal in **Q** space. The new data perfectly agree with the former result; the loss of the incommensurate signal upon heating may explain almost entirely the temperature-dependent contribution to $(1/T_1T)$.[10]

The temperature dependence of the magnetic excitation spectrum at the incommensurate position may be analyzed within the results of the self-consistent renormalization theory described in Ref. 43. In a weakly antiferromagnetic metal the transition is governed by a single parameter related to the Stoner enhancement at the ordering wave vector, $\delta=1-I(\mathbf{q}_i)\chi^0(\mathbf{q}_i)$. The characteristic entities of the magnetic excitations are then given by

$$\kappa^2\propto\delta, \tag{11}$$

$$\Gamma\propto\delta, \tag{12}$$

$$\frac{1}{\chi'(\mathbf{q}_i,0)}\propto\delta. \tag{13}$$

When the system approaches the phase transition, the unique parameter δ diminishes, which behavior should be observable in all three parameters. Equations (11)–(13) imply a sharpening of the magnetic response in **q** space as well as in energy and a divergence of the susceptibility at the

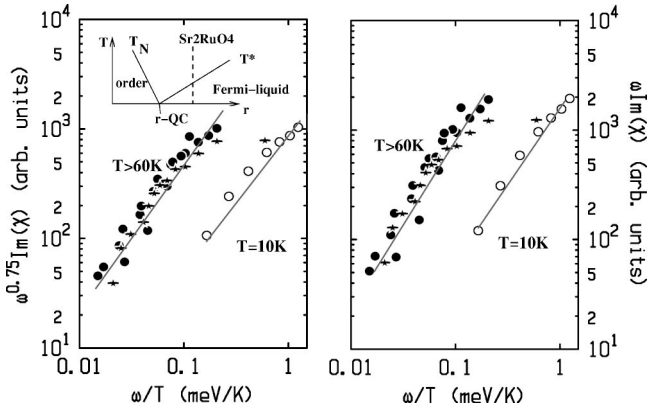

FIG. 8. $\chi''(\mathbf{q}_i,\omega,T)$ multiplied by ω^{α} as a function of ω/T in logarithmic axes; the left and right parts correspond to $\alpha=0.75$ and 1, respectively. The inset gives a schematic representation of a phase diagram close to a quantum critical point. Solid and open circles correspond to the data shown in Fig. 7 and the stars to that of our previous work (Ref. 20).

ordering vector. Fig. 7 qualitatively confirms this picture. All the relevant parameters (see the right scales in Fig. 7) decrease towards low temperature. Therefore, one may conclude that Sr_2RuO_4 is approaching the SDW transition related to the nesting effects upon cooling. However, all these parameters do not vanish completely but remain finite even at the lowest temperatures, in agreement with the well-known fact that Sr_2RuO_4 does not exhibit magnetic ordering. In particular the magnetic scattering remains rather broad in **q** space, implying a short correlation length of just three to four lattice spacings. The temperature dependence of the magnetic excitations corroborates our recent finding that only a small amount of Ti is sufficient to induce SDW magnetic ordering.[35]

Since Sr_2RuO_4 is close to a quantum critical point, it is tempting to analyze whether the excitation spectrum is governed by some ω/T scaling, as has been claimed for the high-temperature superconductor $La_{2-x}Sr_xCuO_4$(Refs. 46–48) and for $CeCu_{5.9}Au_{0.1}$ (Ref. 49). One would expect that the susceptibility is given by

$$\chi''(\mathbf{q}_i,\omega,T)\propto T^{-\alpha}g\left(\frac{\omega}{T}\right). \tag{14}$$

In Fig. 8 we plot the $\omega^{\alpha}\chi''(\mathbf{q}_i,\omega)$ data of Fig. 7 and those obtained previously as a function of temperature[20] against ω/T for $\alpha=0.75$ and 1.0. Only the data at higher temperatures agree with the scaling concept, demonstrating that Sr_2RuO_4 is not a quantum critical point. The schematic inset may illustrate the phase diagram, where the magnetic transition is determined by some parameter *r* (external pressure or composition). At the critical transition one would observe quantum criticality in the entire temperature range, whereas for *r* values where the transition is suppressed quantum criticality is observed only at higher temperatures. One then may expect a crossover temperature T^* where the system transforms from an unconventional metal at high temperatures towards a Fermi liquid at low temperatures.[50] Only in the temperature range above T^* the magnetic excitations should exhibit the related ω/T scaling. Our data clearly show that such scaling can be fitted to the data only for the three higher temperatures studied. The description with the scaling concept seems to be slightly better for the exponent $\alpha=0.75$. The temperature-dependent data suggest a crossover near 30 K. This crossover agrees very well with that seen in electronic transport properties, where well-defined Fermi-liquid behavior is only observed below about 25 K.[1,2]

E. Magnetic scattering in the superconducting phase

As emphasized by Joynt and Rice,[51] the wave-vector- and energy-dependent spin susceptibility in superconductors reflects directly the vector structure of the superconducting (SC) gap function, allowing a complete identification of the SC order parameter symmetry. Inelastic neutron scattering experiments have the potential, in principle, to determine the superconducting order parameter. In high-T_c superconductors, the spin-singlet *d*-wave symmetry SC gap induces a striking modification of the spin susceptibility in the superconducting state. As a consequence, the so-called ''magnetic resonance peak'' has been observed in the superconducting state of various copper oxide superconductors by INS.[52,53] Therefore, a similar experiment in Sr_2RuO_4 would certainly be instructive about the SC gap symmetry.

The enhanced spin susceptibility has been calculated in Refs. 32, 54 and 55, considering a spin-triplet *p*-wave superconductiviting state with $\mathbf{d}(\mathbf{k})=\mathbf{z}(k_x\pm ik_y)$. Note that in such a case, the superconducting gap is isotropic due to the particular shape of the Fermi surface in Sr_2RuO_4. For the wave vector $\mathbf{q}_i$, Kee *et al.*[54] and Morr *et al.*[32] predicted that below T_c spectral weight is shifted from below twice the superconducting gap Δ into a resonancelike feature close to 2Δ. Morr *et al.* find the resonance in the *zz* channel yielding an enhancement of the magnetic excitation intensity by a factor of 9 in the superconducting state as compared to the normal state.[32] The difference between the in-plane and out-of-plane susceptibility in the superconducting state arises from the coherence factor.

Similar theoretical framework is currently used to describe the spin excitation spectrum in spin-singlet HTSC cuprate superconductors.[56] Theoretical works show that the opening of a *d*-wave order gap together with the exchange interaction leads to the appearence of a similar resonant feature below 2Δ at the antiferronagnetic wave vector. These theories successfully account for the observation by INS of the magnetic resonance peak in the superconducting state.

Using unpolarized INS, one measures the superposition of the out-of-plane and in-plane components of the susceptibility [see Eq. (8)] and both components are equally weighted, when performing the measurements $Q_l=0$. Thus, the predicted resonance feature should be observable, at the value of $\sim 2\Delta$, if one obtains an experimental arrangement which allows one to study the inelastic magnetic signal in this energy range. Due to the almost linear decrease of $\chi''(\mathbf{q}_i,\omega)$ towards low energies (see Fig. 7) and due to the higher required resolution which implies less neutron flux, these experiments are extremely time demanding. We have analyzed

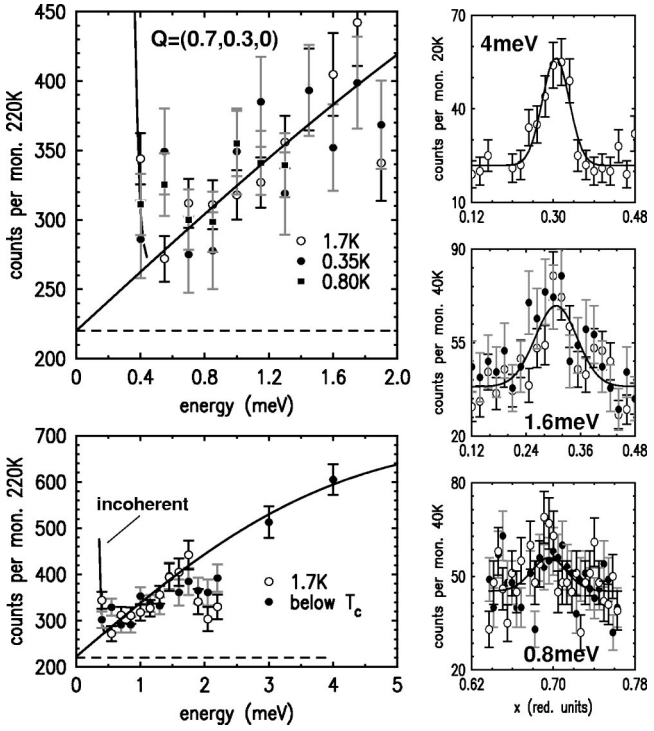

FIG. 9. Results of the experiments performed across the superconducting transition; solid and open symbols correspond to data taken below and above T_c, respectively. The left part shows scans with constant $\mathbf{Q}=(0.7,0.3,0)$ (in the lower part the two low-temperature scans were added), and the right part shows constant energy scans. The horizontal dashed line indicates the background.

the magnetic excitations in the superconducting phase on the cold triple-axis spectrometer IN14 at the ILL using a two-crystal assembly; the results are shown in Fig. 9.

The right part of Fig. 9 shows a scan across the incommensurate peak at $\omega = 4$ meV, i.e., the range already studied with thermal neutrons. This signal can be determined with little beam time. Performing the same scan at 1.6 and 0.8 meV requires considerably more time but still exhibits a well-defined signal which seems not to experience any change in the superconducting state at $T=0.35$ K. The results of constant $\mathbf{Q}$ scans at $\mathbf{Q}=(0.7,0.3,0)$ are shown in the left part of Fig. 9. As there is no visible difference between the results obtained at 0.35 and 0.80 K (both in the SC state), we have added the two scans below T_c in the lower left part of Fig. 9. Importantly and despite efforts to get rather high statistics, there is no change visible in the energy spectra above and below the superconducting transition in the energy range of the superconducting gap. The spin susceptibility is not modified appreciably across the superconducting transition; our data even do not show any opening of a gap. One can describe the energy dependence presented in Fig. 9 with the single relaxor using the same fitted parameters as the low-temperature data in Fig. 5(a). However, the detailed shape of the spin susceptibility (Fig. 9) does not exactly match such a simple linear behavior but rather seems to indicate some anomaly near 2 meV which requires further experimental work.

There is actually little known about the value of the superconducting gap in Sr_2RuO_4. Laube *et al.*[57] have reported an Andreev reflection study where the opening of the gap is clearly visible in an astonishingly large energy range. The quantitative analysis of the spectra is quite involved; assuming a *p*-wave order parameter Laube *et al.* obtain $2\Delta = 2.2$ meV which may be compared to the value expected within BCS theory, $2\Delta = 3.55 k_B T_c = 4.97$ K $= 0.43$ meV. Our data show that there is no change in the excitation spectrum for energies well below the reported value of 2Δ, but it has not been possible to investigate the lowest energies due to the strong elastic incoherent signal. With further increased resolution ($k_f = 1.3$ Å^{-1}) we have scanned the energy range 0.3–0.7 meV at 0.80 K again without evidence of a resonant feature. Furthermore, the comparison of two scans at constant $\mathbf{Q}=(1,0,0)$ did not yield any difference below and above T_c, meaning no ferromagnetic spin susceptibility enhancement.

The theory presented by Morr *et al.*[32] should be considered as being quite reliable in the case of Sr_2RuO_4, since the RPA approach to the magnetic excitations is so successful in the normal state and since Sr_2RuO_4 exhibits well-defined Fermi-liquid properties at temperatures below 25 K. Therefore, the data in Fig. 9 give strong evidence against a simple *p*-wave order parameter in Sr_2RuO_4 with a maximum value of the gap of the order of the reported value.[57] However, in the meanwhile there are several indications that the order parameter is more complex. The recent specific heat data on the highest-quality single crystals[24] point to the existence of line nodes in the gap function which were then shown to be aligned parallel to the a,b plane (horizontal line nodes). Such line nodes were explained by Zhitomirsky and Rice through a proximity effect between the active γ band and the more passive one-dimensional bands.[27] A modulation of the gap function along the c direction will wipe out the resonance predicted for the nonmodulated *p*-wave gap, since for the $\mathbf{Q}$ position analyzed [(0.7 0.3 0)], the electron hole excitation involves parts of the Fermi surface which are fully, partially, or not gapped at all. In this sense the absence of any temperature dependence in the magnetic excitation spectrum is consistent with the presently most accepted shape of the gap function. Further theoretical as well as experimental studies are required to clarify the possibility of a resonant feature at other positions in $(\mathbf{Q},\omega)$ space.

IV. CONCLUSIONS

Using assemblies of several crystals of Sr_2RuO_4 we have analyzed the magnetic excitations by INS. The incommensurate signal arising from the nesting between the one-dimensional bands shows an asymmetry which is well explained by the full RPA analysis as a contribution mainly from the γ band.

The energy dependence of the incommensurate signal varies with temperature and exhibits a general softening of the spectrum upon cooling. This behavior indicates that Sr_2RuO_4 is approaching the corresponding SDW instability at low temperature even though this compound is not at a quantum critical composition. This interpretation is confirmed by the

fact that the generalized susceptibility exhibits some ω/T scaling only above ~ 30 K, i.e., in the temperature range where also the transport properties indicate non-Fermi-liquid behavior.

The analysis of magnetic excitations besides the nesting ones shows only minor contributions. There is some evidence for additional magnetic scattering closer to the zone center but still not peaking at the zone center. This interpretation gets support from the fact that similar scattering is observed in nearly ferromagnetic $Ca_{1.5}Sr_{0.5}RuO_4$ (Ref. 41) and from various RPA calculations which find excitations mainly related to the γ band in this **q** range.

The magnetic excitations in Sr_2RuO_4 may be compared to the distinct types of magnetic order which have been induced by substitution. The dominant excitations reflect the SDW reported to occur in $Sr_2Ru_{1-x}Ti_xO_4$ at small Ti concentrations. The less strong excitations situated more closely to the zone center and most likely related to the γ band become enhanced through Ca substitution which drives the system towards ferromagnetism, but only for rather high Ca concentration.

Upon cooling through the superconducting transition we do not observe any change in the magnetic excitation spectra, which—combined with recent calculations[32]—indicates that the order parameter in Sr_2RuO_4 does not possess simple *p*-wave symmetry. These experimental findings are still in agreement with a *p*-wave order parameter modulated by horizontal line nodes.

ACKNOWLEDGMENTS

We would like to thank O. Friedt, H.Y. Kee, D. Morr, and R. Werner for stimulating discussions and P. Boutrouille (LLB) and S. Pujol (ILL) for technical assistance. Work at Cologne University was supported by the Deutsche Forschungsgemeinschaft through the Sonderforschungsbereich 608. Work at Kyoto was supported by a grant from CREST, Japan Science and Technology Corporation.

*Electronic address: braden@ph2.uni-koeln.de

[1] Y. Maeno, H. Hashimoto, K. Yoshida, S. Nishizaki, T. Fujita, J. G. Bednorz, and F. Lichtenberg, Nature (London) **372**, 532 (1994).
[2] Y. Maeno, K. Yoshida, H. Hashimoto, S. Nishizaki, S.-I. Ikeda, M. Nohara, T. Fujita, A. P. Mackenzie, N. E. Hussey, J. G. Bednorz, and F. Lichtenberg, J. Phys. Soc. Jpn. **66**, 1405 (1997).
[3] A. P. Mackenzie, R. K. W. Haselwimmer, A. W. Tyler, G. G. Lonzarich, Y. Mori, S. Nishizaki, and Y. Maeno, Phys. Rev. Lett. **80**, 161 (1998).
[4] Y. Maeno, T. M. Rice, and M. Sigrist, Phys. Today **54** (1), 42 (2001).
[5] K. Ishida, H. Mukuda, Y. Kitaoka, K. Asayama, Z. Q. Mao, Y. Mori, and Y. Maeno, Nature (London) **396**, 658 (1998).
[6] J. A. Duffy, S. M. Hayden, Y. Maeno, Z. Mao, J. Kulda, and G. J. McIntyre, Phys. Rev. Lett. **85**, 5412 (2000).
[7] G. M. Luke, Y. Fudamoto, K. M. Kojima, M. I. Larkin, J. Merrin, B. Nachumi, Y. J. Uemura, Y. Maeno, Z. Q. Mao, Y. Mori, H. Nakamura, and M. Sigrist, Nature (London) **394**, 558 (1998).
[8] T. M. Rice and M. Sigrist, J. Phys.: Condens. Matter **7**, L643 (1995).
[9] A. Callaghan, C. W. Moeller, and R. Ward, Inorg. Chem. **5**, 1572 (1966); J. M. Longo, P. M. Raccah, and J. B. Goodenough, J. Appl. Phys. **39**, 1372 (1968).
[10] T. Imai, A. W. Hunt, K. W. Thurber, and F. C. Chou, Phys. Rev. Lett. **81**, 3006 (1998).
[11] J. J. Neumeier, M. F. Hundley, M. G. Smith, J. D. Thompson, C. Allgeier, H. Xie, W. Yelon, and J. S. Kim, Phys. Rev. B **50**, 17 910 (1994).
[12] S. Ikeda, Y. Maeno, S. Nkatsuji, M. Kosaka, and Y. Uwatoko, Phys. Rev. B **62**, 6089 (2000); G. Cao, S. McGall, and J. E. Crow, *ibid.* **55**, 672 (1997).
[13] S. Nakatsuji and Y. Maeno, Phys. Rev. Lett. **84**, 2666 (2000).
[14] S. Nakatsuji and Y. Maeno, Phys. Rev. B **62**, 6458 (2000).
[15] S. Nakatsuji (private communication).
[16] M. Braden, G. André, S. Nakatsuji, and Y. Maeno, Phys. Rev. B **58**, 847 (1998).
[17] I. I. Mazin and D. I. Singh, Phys. Rev. Lett. **82**, 4324 (1999).
[18] A. P. McKenzie, S. R. Julian, G. J. McMullan, M. P. Ray, G. G. Lonzarich, Y. Maeno, S. Nishizaki, and T. Fujita, Phys. Rev. Lett. **76**, 3786 (1996).
[19] I. I. Mazin and D. I. Singh, Phys. Rev. Lett. **79**, 733 (1997). Note that the sign of $t_{dd\pi}$ given is wrong.
[20] Y. Sidis, M. Braden, P. Bourges, B. Hennion, S. NishiZaki, Y. Maeno, and Y. Mori, Phys. Rev. Lett. **83**, 3320 (1999).
[21] M. Sato and M. Kohmoto, J. Phys. Soc. Jpn. **69**, 3505 (2000).
[22] T. Kuwabara and M. Ogata, Phys. Rev. Lett. **85**, 4586 (2001).
[23] T. Takimoto, Phys. Rev. B **62**, 14 641 (2000).
[24] S. NishiZaki, Y. Maeno, and Z. Q. Mao, J. Phys. Soc. Jpn. **69**, 572 (2000).
[25] C. Lupien, W. A. MacFarlane, C. Proust, L. Taillefer, Z. Q. Mao, and Y. Maeno, Phys. Rev. Lett. **86**, 5986 (2001).
[26] M. Tanatar, M. Suzuki, S. Nagai, Z. Q. Mao, Y. Maeno, and T. Ishiguro, Phys. Rev. Lett. **86**, 2649 (2001); K. Izawa, H. Takahashi, H. Yamaguchi, Y. Matsuda, M. Suzuki, T. Sasaki, T. Fukase, Y. Yoshida, R. Settai, and T. Onuki, *ibid.* **86**, 2653 (2001).
[27] M. Zhitomirsky and T. M. Rice, Phys. Rev. Lett. **87**, 057001 (2001).
[28] S. W. Lovesey, *Theory of Neutron Scattering from Condensed Matter* (Clarendon, Oxford, 1984), Vol. 2.
[29] T. Nomura and K. Yamada, J. Phys. Soc. Jpn. **69**, 1856 (2000).
[30] K. K. Ng and M. Sigrist, J. Phys. Soc. Jpn. **69**, 3764 (2000).
[31] I. Eremin, D. Manske, C. Joas, and K. H. Bennemann, cond-mat/0102074 (unpublished).
[32] D. Morr, P. F. Trautman, and M. Graf, Phys. Rev. Lett. **86**, 5978 (2001).
[33] A. V. Puchkov, Z. X. Shen, T. Kimura, and Y. Tokura, Phys. Rev. B **58**, 13 322 (1998).
[34] F. Servant, S. Raymond, B. Fak, P. Lejay, and J. Flouquet, Solid State Commun. **116**, 489 (2000).
[35] M. Braden, O. Friedt, Y. Sidis, P. Bourges, M. Minakata, and Y. Maeno, Phys. Rev. Lett. **88**, 197002 (2002).
[36] H. Yoshizawa, T. Kakeshita, R. Kajimoto, T. Tanabe, T. Katsufuji, and Y. Tokura, Phys. Rev. B **61**, 854 (2000).
[37] *International Tables of Crystallography*, edited by A. J. C. Wilson

(Kluwer Academic, Dordrecht, 1995). Note that the form factor for Ru^{4+} is not tabulated.
[38] A. Gukasov and M. Braden (unpublished).
[39] A. Gukasov, M. Braden, R. Papoular, S. Nakatsuji, and Y. Maeno, Phys. Rev. Lett. **89**, 087202 (2002).
[40] Z. Fang and K. Terakura, Phys. Rev. B **64**, 020509 (2001).
[41] O. Friedt and M. Braden (unpublished).
[42] M. Braden, W. Reichardt, S. Nishizaki, Y. Mori, and Y. Maeno, Phys. Rev. B **57**, 1236 (1998).
[43] T. Moriya, *Spin Fluctuations in Itinerant Electron Magnetism*, Solid-State Sciences Vol. 56 (Springer-Verlag, Berlin, 1985).
[44] M. G. Hildebrand, M. Reedyk, T. Katsufuji, and Y. Tokura, Phys. Rev. Lett. **87**, 227002 (2001).
[45] C. Berthier *et al.*, J. Phys. I **6**, 2205 (1996); R. E. Walstedt, B. S. Shastry, and S. W. Cheong, Phys. Rev. Lett. **72**, 3610 (1994).
[46] G. Aeppli, T. E. Mason, S. M. Hayden, H. A. Mook, and J. Kulda, Science **278**, 1432 (1997).
[47] B. Keimer, R. J. Birgeneau, A. Cassanho, Y. Endoh, R. W. Erwin, M. A. Kastner, and G. Shirane, Phys. Rev. Lett. **67**, 1930 (1991).
[48] S. Sachdev and J. Ye, Phys. Rev. Lett. **69**, 2411 (1992).
[49] A. Schroeder, G. Aeppli, E. Bucher, R. Ramazashvili, and P. Coleman, Phys. Rev. Lett. **80**, 5623 (1998).
[50] S. Sachdev, Science **288**, 475 (2000).
[51] R. Joynt and T. M. Rice, Phys. Rev. B **38**, 2345 (1988).
[52] J. Rossat-Mignod, L. P. Regnault, C. Vettier, P. Bourges, P. Burlet, J. Bossy, J. Y. Henry, and G. Lapertot, Physica C **185-189**, 86 (1991).
[53] H. F. He, P. Bourges, Y. Sidis, C. Ulrich, L. P. Regnault, S. Pailhès, N. S. Berzigiarova, N. N. Kolesnikov, and B. Keimer, Science **295**, 1045 (2002), and references therein.
[54] H. Y. Kee, J. Phys.: Condens. Matter **12**, 2279 (2000).
[55] D. Fay and L. Tewordt, Phys. Rev. B **62**, 4036 (2000).
[56] See, e.g., F. Onufrieva and P. Pfeuty, Phys. Rev. B **65**, 054515 (2002).
[57] F. Laube, G. Goll, H. v. Löhneysen, M. Fogelström, and F. Lichtenberg, Phys. Rev. Lett. **84**, 1595 (2000).